Effect of the dielectric constant of a liquid electrolyte on lithium metal anodes

Ju Young Kim[a,*], Dong Ok Shin[a], Taeyong Chang[b], Kwang Man Kim[a], Jiseon Jeong[c], Joonam Park[d], Yong Min Lee[d], Kuk Young Cho[e], Charudatta Phatak[f], Seungbum Hong[b], Young-Gi Lee[a,*]

[a]*Research Group of Multidisciplinary Sensors, Electronics and Telecommunications Research Institute (ETRI), Daejeon 34129, Republic of Korea*

[b]*Department of Materials Science and Engineering, Korea Advanced Institute of Science and Technology (KAIST), Daejeon 34141, Republic of Korea*

[c]*Research Division, EnChem Co., Ltd., Cheon-an 31214, Republic of Korea*

[d]*Department of Energy Science and Engineering, Daegu Gyeongbuk Institute of Science and Technology (DGIST), Daegu 42988, Republic of Korea*

[e]*Deparment of Materials Science and Chemical Engineering, Hanyang University, Ansan 15588, Republic of Korea*

[f]*Materials Science Division, Argonne National Laboratory, Lemont, IL 60439, USA*

*Corresponding authors.

E-mail address: juyoung@etri.re.kr (J.Y. Kim), lyg@etri.re.kr (Y.-G. Lee).

Highlights

- Electric field intensity for lithium plating is derived from interface analysis.
- Electrolytes with different dielectric constants are designed systematically.
- Confirmed enhanced cycling performance of lithium occurs with high EC content.

Abstract

Lithium metal is considered one of the most promising anode materials for realizing high volumetric and gravimetric energy density, owing to the high specific capacity (~3860 mAh g^{-1}) and the low electrochemical potential of lithium (–3.04 V vs. the standard hydrogen electrode). However, undesirable dendritic lithium growth and corresponding instability of the solid electrolyte interphase prevent safe and long-term use of lithium metal anodes. This paper presents a simple electrolyte approach to enhance the performance of lithium metal batteries by tuning the dielectric constant of the liquid electrolyte. Electrolyte formulations are designed by changing the concentration of ethylene carbonate to have various dielectric constants. This study confirms that high ethylene carbonate content in a liquid electrolyte enhances the cycling performance of lithium metal batteries because the electric field intensity applied to the electrolyte is reduced in relation to the polarization of the electrolyte and thus allows smooth lithium plating and formation of a stable solid electrolyte interphase. We believe that this approach provides an important concept for electrolyte system design suitable to lithium metal batteries.

Keywords: lithium metal secondary batteries; lithium metal anode; electrolyte; dielectric constant.

1. Introduction

High-energy-density storage devices are in great demand for emerging and advanced applications such as electric vehicles and energy storage systems [1-6]. Utilizing lithium metal as an anode material instead of the graphite used in conventional lithium ion batteries, lithium metal secondary batteries make it possible to realize higher energy density through the high specific capacity of lithium (~3860 mAh g^{-1}) and its low electrochemical potential (–3.04 V vs. the standard hydrogen electrode). However, in contrast to the structurally stable operation of graphite anodes, the host-less reaction mechanism of lithium metal anodes inevitably induces unstable dendritic deposition and formation of mossy structures along with continuous consumption of the electrolyte [7-10]. This undesirable complex lithium structure eventually increases the overpotential in the lithium plating/stripping step and formation of electrochemically inactive dead lithium, which are closely related to degradation of cell performance and undesirable explosion events [8, 11]. Ultimately, preventing this undesirable lithium structure is essential for extending the stable operation of lithium metal secondary batteries.

In this regard, many novel strategies, such as hybrid polymeric electrolytes and electrolyte design, have been developed [12-23], among which one of the major ways to suppress dendritic lithium growth is to induce locally reduced current density [24]. Generally, dendritic lithium growth is strongly influenced by kinetics rather than by thermodynamics [25, 26]. Thus, charging at higher current density leads to even greater formation of the undesirable complex structure, preventing the deposition of dense lithium [10, 27, 28]. To exploit this concept, a host-electrode design has been proposed to reduce the local current density [24, 29-34]. The current density is inversely proportional to the surface area of an electrode under charge/discharge conditions at a constant current. Therefore, we reasoned that fabrication of three-dimensional (3D) porous electrodes with macroscopic high conductivity and high surface area could successfully lower the local effective current density [24]. This would reduce the electric field intensity due to almost constant conductivity ($J = \sigma E$, where J is the current density, σ is the conductivity, and E is the electric field intensity), and enable stable lithium plating/stripping with

low overpotential and enhanced cycling performance.

Herein, we report a simple method for reducing the electric field intensity applied to the electrolyte using electrolyte design to enhance the performance of a lithium metal anode. The fundamental parameter to be controlled in our cell design is the dielectric constant of the electrolyte, which mainly participates in the dissociation of lithium salt. Common and versatile, ethylene carbonate (EC) was utilized to modify the dielectric constant in the liquid electrolyte. Thus, several electrolytes with different dielectric constants were designed and their electrochemical performances in configurations of a lithium symmetric cell and a full cell were compared, along with solid electrolyte interphase (SEI) analysis. These results confirmed that electrolyte containing a high content of EC with a high dielectric constant promoted stable lithium plating/stripping and improved cycling performance.

To reduce the electric field intensity, we applied the governing principle of using the boundary condition for the electrostatic field at the interface between the lithium metal and the liquid electrolyte (Figure 1a). As is well known in electromagnetics, the equation below is valid at the interface between media with different physical properties [35]:

$$(D_1 - D_2) \cdot n = \varrho \tag{1}$$

where D_1 and D_2 are the electric displacement in medium 1 and medium 2, respectively; n is the normal unit vector to the interface; ϱ is the volume density of the free charge. In general, when current is applied to a lithium metal contact in a liquid electrolyte, electric displacement in each medium should be nearly zero because both are conductors. However, an electrochemical reaction occurs for lithium plating, which consumes the lithium ions near the lithium metal surface. In this way, a depletion layer is formed in the liquid electrolyte owing to the diffusion-limited behavior of lithium ions [10]. This layer can be described as an interface between the metal and dielectric media (Figure 1b). In this situation, owing to $D_{lithium} \approx 0$ in the metal medium, the electric displacement in the liquid electrolyte is

$$D_{electrolyte} \approx \varrho \tag{2}$$

which can also be expressed as

$$E_{electrolyte} \approx \varrho / \varepsilon_{electrolyte} \quad (3)$$

This means that the electric field applied to the electrolyte is inversely proportional to its dielectric constant. Therefore, we concluded that proper design of the electrolyte in terms of its dielectric constant would contribute to reduction of the electric field intensity involved in lithium plating, thus suppressing dendritic lithium growth.

2. Experimental

Electrolyte solutions of 1.0 M $LiPF_6$ dissolved in ethylene carbonate (EC)/dimethyl carbonate (DMC) with different blending ratios (2/8, 5/5, and 8/2 by volume ratio) were provided by Enchem Co., Ltd. Lithium metal foils (100 and 20 μm thickness) were purchased from Honjo Metal Co. and were used without additional treatment. The alumina (Al_2O_3)-coated separator and conventional polyolefin separator were purchased from MTI Co. and Asahi Kasei, respectively. Commercially available $LiCoO_2$ (Umicore, D_{50} = 10 μm), carbon black (Imerys), and poly(vinylidene fluoride: PVDF) (Aldrich) were also used to fabricate the cathode electrode.

To measure the ionic conductivity of electrolytes, a lithium ion blocking cell configuration comprising two parallel stainless steel electrodes was fabricated and a frequency response analyzer (Solatron HF 1225 Gain-Phase Analyzer) in the frequency range of $10^{-1} \sim 10^5$ Hz was utilized. The linear sweep voltammetry (Solatron 1470E Cell Test System) was used to evaluate the electrochemical stability of electrolytes. The cell consisted of working electrode (stainless steel plate), counter electrode (lithium metal), Al_2O_3-coated separator, and each electrolyte. The viscosity of electrolytes was measured by a viscosity meter (A&D SV-10). The microscopic morphology of the lithium metal surface was observed using a Scanning Electron Microscope (SEM) (Hitachi S-4800). The X-ray photoelectron spectroscopy (XPS) (Thermo VG Scientific K-alpha) measurement was conducted for the elemental analysis of SEI on cycled lithium metal surface.

For the lithium symmetric cell, 100 μm thick lithium metal was used for both electrodes. An

Al_2O_3-coated separator was utilized along with liquid electrolyte of various compositions (EC/DMC 2/8, 5/5, and 8/2 by volume ratio). In the configuration of the lithium metal full cell, relatively thin lithium metal (20 μm) on a copper current collector was used. For fabrication of the cathode, a slurry of $LiCoO_2$, carbon black, PVdF (92:4:4 wt%) in an *N*-methyl-2-pyrrolidone/acetone mixture (1:1 by volume ratios) was coated onto an Al current collector using a doctor blade apparatus. A cathode was prepared with an areal capacity of ~1.3 mAh cm^{-2}. For the electrolyte and separator, identical processes were performed as for the lithium symmetric cell. All cells were fabricated as pouch types with active areas of 2 × 2 cm. Prior to cycling, aging for three days was done to ensure complete wetting with the electrolyte of the separator and the cathode. In addition, the formation (pre-cycling) at the rate of 0.1 C for 3 cycles was performed in advance. The electrochemical performance of the symmetric and full cells was investigated under various charge/discharge conditions using a cycle tester (Toyo System).

3. Results and discussion

To minimize the effect of the electrochemical reaction of the electrolyte on the lithium metal, identical chemical species were selected to make up the model electrolyte, but they had different volumetric blending ratios. To prepare a high dielectric constant solvent, EC with a dielectric constant of 95.3 at 25 °C was used, and DMC with a dielectric constant of 3.08 at 25 °C was utilized to control the final dielectric constant of the electrolyte [36]. Three combinations of EC/DMC (2/8, 5/5, and 8/2 by volume ratio) were prepared and their calculated dielectric constants were 21.5, 49.2, and 76.9, respectively, based on a simple linear mixing model. There was a slight deviation from the precise values of the dielectric constants in the solvent blend system containing lithium salt, but the overall trend in the change of the dielectric constant in relation to the mixtures is still valid [36, 37].

For lithium ionic transport, 1.0 M $LiPF_6$ salt was dissolved in each mixture and their basic properties, such as ionic conductivity, viscosity and transference number, were measured. The ionic conductivity of EC/DMC 8/2 had a relatively low value (9.55 mS cm^{-1}) due to its high viscosity (5.61 cP) while others exhibited reasonable values (11.52 mS cm^{-1}, 3.69 cP for EC/DMC 5/5 and 11.85 mS

cm^{-1}, 2.49 cP for EC/DMC 2/8). However, when the conventional hydrophobic olefin separator and aging for 3 days at room temperature was used for cell fabrication, the ionic conductivity of the electrolyte with EC/DMC 8/2 was significantly low (0.88 μS cm^{-1}) due to the low wettability of the hydrophobic separator with this electrolyte (EC/DMC 8/2) (Figures S1 and S2). In contrast, an Al_2O_3-coated separator introduced as a hydrophilic separator enabled moderate wettability with the polar electrolyte. Thus, with the surface energy modified separator, the wetting property of the electrolyte with EC/DMC 8/2 was improved, exhibiting a reasonable ionic conductivity of 0.11 mS cm^{-1} (Figure S3) [38]. Using this separator, the lithium ion transference number of each electrolyte was calculated in a lithium ion conducting configuration, and they indicated similar values (0.24, 0.27, and 0.22 for EC/DMC 2/8, 5/5, and 8/2, respectively) (Figure S4) [39]. For the electrochemical stability of each electrolyte, a wider electrochemically stable window was obtained using an electrolyte with a higher content of EC (Figure 1c), which would be advantageous for assembly with high voltage cathode materials to realize a battery system with higher energy density.

Utilizing the Al_2O_3-coated separator, lithium symmetric cells with lithium metal (~100 μm thick) and the electrolytes were fabricated as pouch-type cells with an active area of 4 cm^2. The lithium symmetric cell is an appropriate model for evaluating lithium metal performance excluding the cathode effect. The lithium plating/stripping was performed at 2 mA cm^{-2} for 30 min. Interestingly, the cycling performance of the cell with the electrolyte with EC/DMC 8/2 was superior to the others (Figure 1d). For the cells with the electrolyte with EC/DMC 2/8 and 5/5, the voltage profiles abruptly increased after ~46 and ~92 h, respectively (Figures 1e and 1f). The cell with the electrolyte with EC/DMC 8/2 showed stable operation for ~138 h and cell failure after that. Consistent results were obtained at 1 mA cm^{-2} for 1 h (Figure S5). Despite superior performance of the cell with the electrolyte with EC/DMC 8/2, the measured voltage of the cell with the electrolyte with EC/DMC 8/2 during the plating/stripping was not significantly lower than the others (Figure 1d-f), which might be related to low ionic conductivity of the electrolyte with EC/DMC 8/2 (Figure S3). The measured cell voltage is expressed as the equation below.

$$V_{cell} = V_{oc} + IR + \eta \quad (4)$$

where V_{cell} is the measured cell voltage, V_{oc} is the open-circuit voltage, IR is the voltage drop by internal resistance, and η is the overpotential [7]. By simple calculations based on the impedance measurement of each electrolyte, the IR drops of EC/DMC 2/8, 5/5, and 8/2 at 2 mA cm^{-2} were roughly ~7.4, 8.3, and 44 mV, respectively (active area: 4 cm^2) (Figure S3). Considering this tendency for an IR drop effect, the actual overpotential at the cell with the electrolyte with EC/DMC 8/2 may be lower than the others, which creates enhanced, more stable cycling performance in a lithium symmetric cell. Regarding the whole shape of the charge/discharge curve, our cells follow a dynamic change of voltage similar to the one proposed by Dasgupta et al. [7, 9]. Therefore, we considered that the nucleation or growth of dendrites on the cathode and electrodissolution from dendrites, bulk surface or pits on the anode could occur in our cells, depending on the energy barriers of each step. It is remarkable that the pitting phenomenon was more delayed with a higher content of EC, which is highly advantageous for long-term use of lithium metal (Figures 1d-f) [7].

We observed the microscopic morphologies of cycled lithium electrodes in relation to the electrolytes using SEM. After disassembly of the cells after 15 cycles (2 mA cm^{-2} for 30 min), the lithium electrode was washed with DMC to remove traces of the electrolyte and dried in a vacuum. As shown in Figure 2, there were many dendritic and mossy structures on the lithium surface cycled in the electrolyte with a low dielectric constant (EC/DMC 2/8). Less of the undesirable lithium structure was confirmed in cells with a higher dielectric constant electrolyte (EC/DMC 5/5 and 8/2). Moreover, the lithium domain morphologies plated in the EC/DMC 8/2 electrolyte were larger than those in EC/DMC 5/5 (Figures 2d and 2f). This was caused by the inverse relationship between the size of the nuclei and the overpotential, which may have been the reason for a decrease of the electric field intensity by the high dielectric constant of the electrolyte [40]. Eventually, such a relatively uniform and dense lithium structure in the electrolyte with a high dielectric constant might contribute to long-term use of the lithium by reducing the overpotential increase during cycling [7-9]. After the cell failure, we also observed the morphologies of lithium metal by SEM. As shown in Figure 3, we confirmed that for all

electrolyte compositions, the dense lithium metal turned into the mossy structure, which might be a major factor to induce the cell failure than a short circuit by lithium dendrites.

X-ray photoelectron spectroscopy (XPS) of the cycled lithium metal surfaces was performed to analyze precisely the SEI depending on the electrolyte composition. Despite the use of identical chemical species (EC and DMC), the SEI composition became different depending on the EC concentration. According to previous reports [41], as the EC concentration decreases, the inorganic, Li^+-permeable carbonate is enriched in SEI, which is known to be suitable for long-term use of a lithium metal anode [27, 42, 43]. The XPS results in Figures 4a–c and g are consistent with previous work. For the sample using EC/DMC 2/8, there was a higher content of the inorganic carbonyl group (~289.0 eV in the C 1s spectrum) than that in the others [44, 45]. In the F 1s spectra in Figures 3d–f and h, more LiF (~684.8 eV in F 1s spectrum) was formed in cells with a higher EC/DMC ratio [46], which may have been caused by the favorable SEI formation dependent on the current density [47]. We inferred that the electric field intensity reduced by polarization of the electrolyte induced decreased repulsion of PF_6^- from the lithium surface. Thus, more of the PF_6^- existing near the lithium electrode could participate in SEI formation. In addition, because the EC solvated PF_6^- contributing to SEI formation is abundant in a high EC concentrated electrolyte, it might affect the formation of LiF-enriched SEI [48]. Many researchers have investigated better components in SEI for lithium metal anodes, and recent results have focused on LiF SEI in terms of large band gap energy (13.6 eV) and wide electrochemical stability [46, 49-51], even though Li_2CO_3 and LiF are generally favorable for SEI in lithium metal anodes [27, 43]. Regarding SEI conduction, the cycled cell with EC/DMC 2/8 exhibited the lowest resistance of all, but the others showed reasonable conduction for lithium ion transport (Figure S6). Considering analysis of the cycling result (Figure 1d), we anticipate that the enhanced cycling performance in the lithium metal anode was affected by the reduced electric field via the high concentration of EC with a high dielectric constant and resulting favorable formation of LiF-enriched SEI.

The pouch-type full-cells consisting of thin lithium metal (~20 μm) and $LiCoO_2$ were assembled with each electrolyte, and their cycling performance was measured at the charge/discharge

rate of 0.5 C. The relatively thin lithium metal thickness (~20 μm) was reasonably comparable with that of a conventional graphite anode for realizing the high volumetric energy density. As shown in Figure 5a, superior performance of the full cell with EC/DMC 8/2 was confirmed by comparison with the others, which was consistent with the results for the lithium symmetric cell in Figure 1d. For the full cell with EC/DMC 2/8, rapid cell failure occurred after ~10 cycles, while the full cell with EC/DMC 8/2 exhibited stable cycling for 45 cycles. Quantitatively, ~80% retention of the discharging capacity was confirmed at 9, 39, and 54 cycles for EC/DMC 2/8, 5/5, and 8/2, respectively. The Coulombic efficiency of the cell also showed tendencies similar to cycling performance, as shown in Figure 5b.

4. Conclusions

In summary, we examined the effect of the dielectric constant of a liquid electrolyte on lithium metal anodes. Liquid electrolytes with different dielectric constants were systematically designed by controlling the concentration of EC with large polarization, along with controlled surface polarity of the separator. Our study confirmed that an electrolyte with a high dielectric constant containing high EC content could suppress dendritic lithium growth and enable more stable cycling performance. This was mainly due to a decrease in the electric field intensity by large polarization of the electrolyte and corresponding stable SEI formation, which may be a considerable factor in the analysis of lithium metal secondary batteries. Moreover, with this electrolyte design principle we can expect that novel electrolytes suitable for lithium metal secondary batteries might be realized by synthesizing new organic species or by reviewing diverse previously used solvents. In addition, by virtue of the good compatibility of the electrolyte approach with previous research, this advanced electrolyte design will exhibit a synergistic effect that will prolong the use of lithium metal, including 3D conductive scaffolds for lithium hosting, artificial SEI, and functional electrolyte additives.

Acknowledgements

This work was supported by Technology Development Program to Solve Climate Changes of the National Research Foundation (NRF) funded by the Ministry of Science & ICT (2017M1A2A2044492), and R&D Convergence Program (14-02-KITECH) of the National Research Council of Science and Technology (NST) of Korea.

Appendic A. Suppliementary data

Supplementary data associated with this article can be found, in the online version, at XXXX

References

[1] W. Xu, J. Wang, F. Ding, X. Chen, E. Nasybulin, Y. Zhang, J.-G. Zhang, Energy Environ. Sci., 7 (2014) 513-537.

[2] J.W. Choi, D. Aurbach, Nat. Rev. Mater., 1 (2016) 16013.

[3] K. Zhang, G.-H. Lee, M. Park, W. Li, Y.-M. Kang, Adv. Energy Mater., 6 (2016) 1600811.

[4] Y. Guo, H. Li, T. Zhai, Adv. Mater., 29 (2017) 1700007.

[5] D. Lin, Y. Liu, Y. Cui, Nat. Nanotech., 12 (2017) 194-206.

[6] H. Zhao, N. Deng, J. Yan, W. Kang, J. Ju, Y. Ruan, X. Wang, X. Zhuang, Q. Li, B. Cheng, Chem. Eng. J., 347 (2018) 343-365.

[7] K.N. Wood, E. Kazyak, A.F. Chadwick, K.-H. Chen, J.-G. Zhang, K. Thornton, N.P. Dasgupta, ACS Cent. Sci., 2 (2016) 790-801.

[8] D. Lu, Y. Shao, T. Lozano, W.D. Bennett, G.L. Graff, B. Polzin, J. Zhang, M.H. Engelhard, N.T. Saenz, W.A. Henderson, P. Bhattacharya, J. Liu, J. Xiao, Adv. Energy Mater., 5 (2015) 1400993.

[9] K.-H. Chen, K.N. Wood, E. Kazyak, W.S. LePage, A.L. Davis, A.J. Sanchez, N.P. Dasgupta, J. Mater. Chem. A, 5 (2017) 11671-11681.

[10] P. Bai, J. Li, F.R. Brushett, M.Z. Bazant, Energy Environ. Sci., 9 (2016) 3221-3229.

[11] J.R. Nair, M. Destro, F. Bella, G.B. Appetecchi, C. Gerbaldi, J. Power Sources, 306 (2016) 258-267.

[12] F. Ding, W. Xu, G.L. Graff, J. Zhang, M. Sushko, X. Chen, J. Am. Chem. Soc., 135 (2013) 4450-4456.

[13] J. Qian, B.D. Adams, J. Zheng, W. Xu, W.A. Henderson, J. Wang, M.E. Bowden, S. Xu, J. Hu, J.-G. Zhang, Adv. Funct. Mater., 26 (2016) 7094-7102.

[14] Z. Liang, G. Zheng, C. Liu, N. Liu, W. Li, K. Yan, H. Yao, P.C. Hsu, S. Chu, Y. Cui, Nano Lett., 15 (2015) 2910-2916.

[15] M.H. Ryou, D.J. Lee, J.N. Lee, Y.M. Lee, J.K. Park, J.W. Choi, Adv. Energy Mater., 2 (2012) 645-650.

[16] J. Park, J. Jeong, Y. Lee, M. Oh, M.-H. Ryou, Y.M. Lee, Adv. Mater. Interfaces, 3 (2016) 1600140.

[17] X.-X. Zeng, Y.-X. Yin, N.-W. Li, W.-C. Du, Y.-G. Guo, L.-J. Wan, J. Am. Chem. Soc., 138 (2016) 15825-15828.

[18] E. Cha, M.D. Patel, J. Park, J. Hwang, V. Prasad, K. Cho, W. Choi, Nat. Nanotech., 13 (2018) 337-344.

[19] H. Lee, X. Ren, C. Niu, L. Yu, M.H. Engelhard, I. Cho, M.-H. Ryou, H.S. Jin, H.-T. Kim, J. Liu, W. Xu, J.-G. Zhang, Adv. Funct. Mater., 27 (2017) 1704391.

[20] S. Suriyakumar, S. Gopi, M. Kathiresan, S. Bose, E.B. Gowd, J.R. Nair, N. Angulakshmi, G. Meligrana, F. Bella, C. Gerbaldi, A.M. Stephan, Electrochim. Acta, 285 (2018) 355-364.

[21] N.N.M. Radzir, S.A. Hanifah, A. Ahmad, N.H. Hassan, F. Bella, J. Solid State Electrochem., 19 (2015) 3079-3085.

[22] Y. Chen, Y. Tian, Z. Li, N. Zhang, D. Zeng, G. Xu, Y. Zhang, Y. Sun, H. Ke, H. Cheng, Journal of Membrane Science, 566 (2018) 181-189.

[23] J.R. Nair, L. Porcarelli, F. Bella, C. Gerbaldi, ACS Appl. Mater. Interfaces, 7 (2015) 12961-12971.

[24] R. Zhang, X.-B. Cheng, C.-Z. Zhao, H.-J. Peng, J.-L. Shi, J.-Q. Huang, J. Wang, F. Wei, Q. Zhang, Adv. Mater., 28 (2016) 2155-2126.

[25] J.N. Chazalviel, Phys. Rev. A, 42 (1990) 7355-7367.

[26] C. Monroe, J. Newman, J. Electrochem. Soc., 150 (2003) A1377-A1384.
[27] S.M. Wood, C.H. Pham, R. Rodriguez, S.S. Nathan, A.D. Dolocan, H. Celio, J.P. de Souza, K.C. Klavetter, A. Heller, C.B. Mullins, ACS Energy Lett., 1 (2016) 414-419.
[28] G. Lian, O. Gerko, R. Aleksandar, M.H. Peter, C.S. Peter, J. Phys. D: Appl. Phys., 44 (2011) 443001.
[29] Q. Yun, Y.-B. He, W. Lv, Y. Zhao, B. Li, F. Kang, Q.-H. Yang, Adv. Mater., 28 (2016) 6932-6939.
[30] T.-T. Zuo, X.-W. Wu, C.-P. Yang, Y.-X. Yin, H. Ye, N.-W. Li, Y.-G. Guo, Adv. Mater., 29 (2017) 1700389.
[31] L.-L. Lu, J. Ge, J.-N. Yang, S.-M. Chen, H. Yao, F. Zhou, S.-H. Yu, Nano Lett., 16 (2016) 4431-4437.
[32] C.-P. Yang, Y.-X. Yin, S.-F. Zhang, N.-W. Li, Y.-G. Guo, Nat. Commun., 6 (2015) 8058.
[33] D. Lin, Y. Liu, Z. Liang, H.-W. Lee, J. Sun, H. Wang, K. Yan, J. Xie, Y. Cui, Nat. Nanotech., 11 (2016) 626-633.
[34] A.-R.O. Raji, R. Villegas Salvatierra, N.D. Kim, X. Fan, Y. Li, G.A.L. Silva, J. Sha, J.M. Tour, ACS Nano, 11 (2017) 6362-6369.
[35] C. David K., Field and Wave Electromagnetics, Addison Wesley, 1989.
[36] D.S. Hall, J. Self, J.R. Dahn, J. Phys. Chem. C, 119 (2015) 22322-22330.
[37] A. Levy, D. Andelman, H. Orland, Phys. Rev. Lett., 108 (2012) 227801.
[38] M.H. Ryou, Y.M. Lee, J.K. Park, J.W. Choi, Adv. Mater., 23 (2011) 3066-3070.
[39] S. Zugmann, M. Fleischmann, M. Amereller, R.M. Gschwind, H.D. Wiemhöfer, H.J. Gores, Electrochim. Acta, 56 (2011) 3926-3933.
[40] A. Pei, G. Zheng, F. Shi, Y. Li, Y. Cui, Nano Lett., 17 (2017) 1132-1139.
[41] Y. Wang, S. Nakamura, M. Ue, P.B. Balbuena, J. Am. Chem. Soc., 123 (2001) 11708-11718.
[42] S. Shi, Y. Qi, H. Li, L.G. Hector, J. Phys. Chem. C, 117 (2013) 8579-8593.
[43] X.-B. Cheng, R. Zhang, C.-Z. Zhao, Q. Zhang, Chem. Rev., 117 (2017) 10403-10473.
[44] J. Zheng, M.H. Engelhard, D. Mei, S. Jiao, B.J. Polzin, J.-G. Zhang, W. Xu, Nat. Energy, 2 (2017) 17012.
[45] P. Verma, P. Maire, P. Novák, Electrochim. Acta, 55 (2010) 6332-6341.
[46] X.-Q. Zhang, X.-B. Cheng, X. Chen, C. Yan, Q. Zhang, Adv. Funct. Mater., 27 (2017) 1605989.
[47] K. Kanamura, S. Shiraishi, Z.i. Takehara, J. Electrochem. Soc., 143 (1996) 2187-2197.
[48] A. von Wald Cresce, M. Gobet, O. Borodin, J. Peng, S.M. Russell, E. Wikner, A. Fu, L. Hu, H.-S. Lee, Z. Zhang, X.-Q. Yang, S. Greenbaum, K. Amine, K. Xu, J. Phys. Chem. C, 119 (2015) 27255-27264.
[49] S. Li, M. Jiang, Y. Xie, H. Xu, J. Jia, J. Li, Adv. Mater., 30 (2018) 1706375.
[50] S. Choudhury, L.A. Archer, Adv. Electron. Mater., 2 (2016) 1500246.
[51] L. Fan, H.L. Zhuang, L. Gao, Y. Lu, L.A. Archer, J. Mater. Chem. A, 5 (2017) 3483-3492.

Figure captions

Figure 1. a) Schematic illustration of a lithium/liquid electrolyte interface. b) Free charge concentration profile for lithium deposition step at the interface of the lithium and the liquid electrolyte. c) Linear sweep voltammetry of electrolytes with EC/DMC 2/8, 5/5, and 8/2. d) Galvanostatic cycling voltage profile for lithium symmetric cells with different electrolyte compositions (EC/DMC 2/8, 5/5, and 8/2) at 2 mA cm^{-2} (1 mAh cm^{-2}) and enlarged images of e) 35–50 h, and f) 90–105 h.

Figure 2. 60°-tilted SEM images of the lithium surface after 15 cycles (2 mA cm^{-2}, 1 mAh cm^{-2}), operated in a liquid electrolyte using EC/DMC (a, b) 2/8, (c, d) 5/5, and (e, f) 8/2 in the lithium symmetric cells.

Figure 3. 60°-tilted SEM images of lithium surface after a cell failure (2 mA cm^{-2}, 1 mAh cm^{-2}), operated in liquid electrolytes with EC/DMC 2/8, 5/5, and 8/2.

Figure 4. XPS spectra of C 1s, F 1s for lithium surface operated in a liquid electrolyte using EC/DMC (a, d) 2/8, (b, e) 5/5, and (c, f) 8/2. These cells were evaluated after 5 cycles (0.5 mA cm^{-2} for 10 min). g, h) Percentage of each component of SEI depending on EC/DMC blending ratio, based on XPS analysis.

Figure 5. a) Cycling performance and b) Coulombic efficiency of a lithium-$LiCoO_2$ full cell with different electrolytes (EC/DMC 2/8, 5/5, and 8/2) (lithium thickness = ~20 μm).

Figure 1

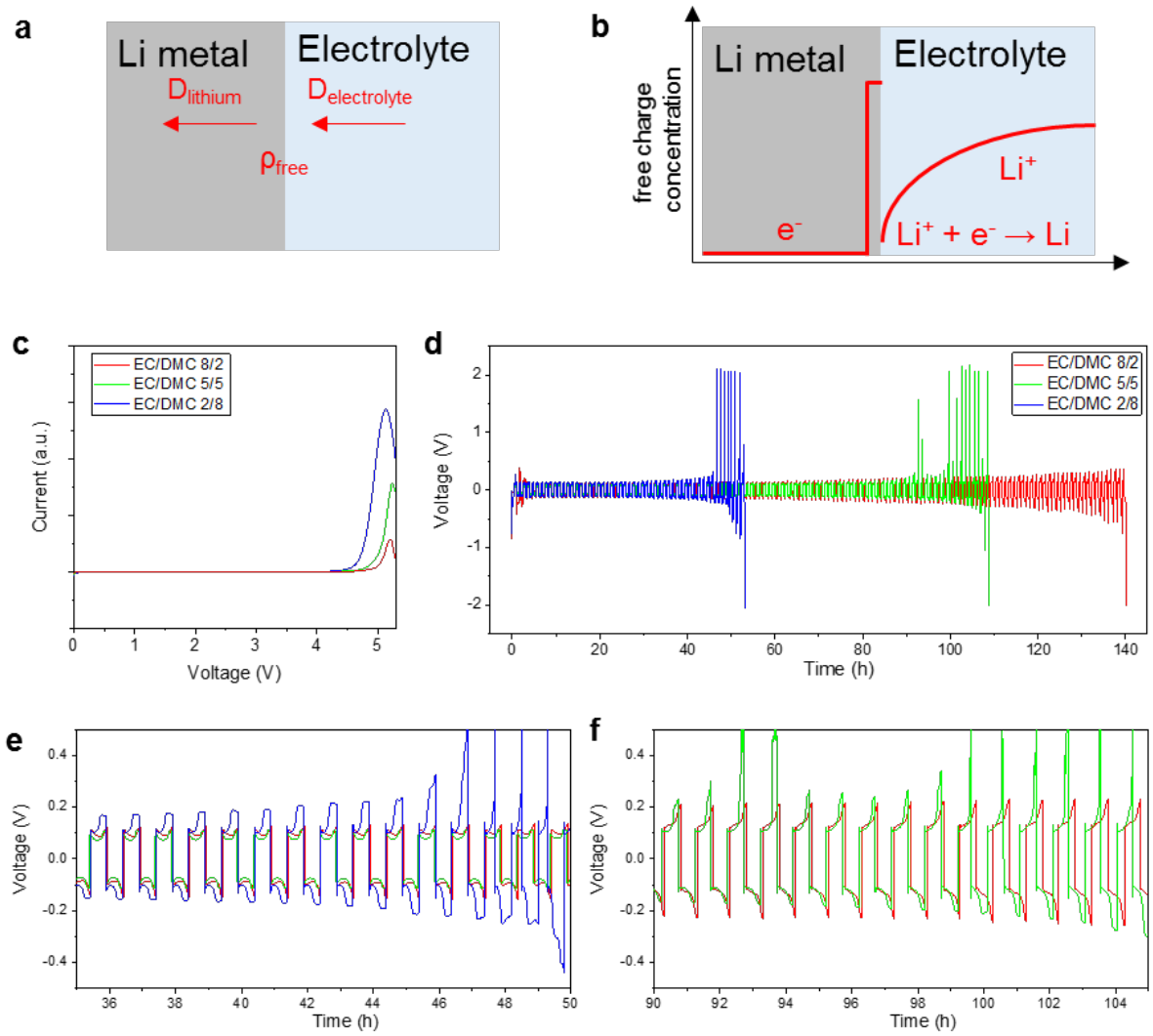
a
Li metal
Electrolyte
D lithium
D electrolyte
ρ free
b
free charge concentration
Li metal
Electrolyte
Li+
e-
Li+ + e- → Li
c
EC/DMC 8/2
EC/DMC 5/5
EC/DMC 2/8
Current (a.u.)
Voltage (V)
d
EC/DMC 8/2
EC/DMC 5/5
EC/DMC 2/8
Voltage (V)
Time (h)
e
Voltage (V)
Time (h)
f
Voltage (V)
Time (h)

Figure 2

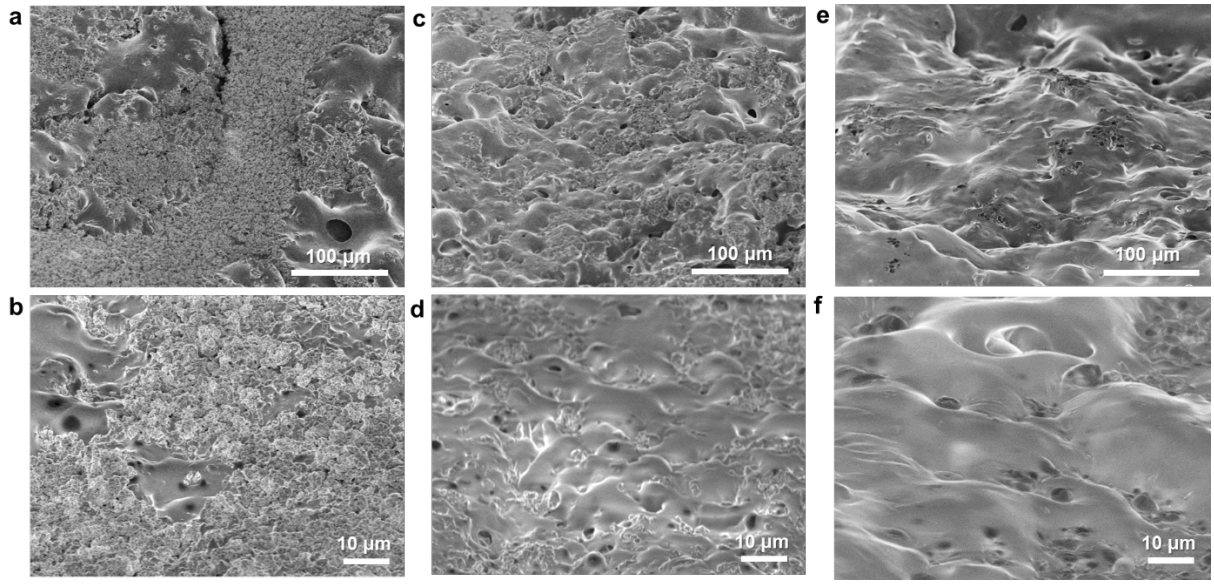

Figure 3

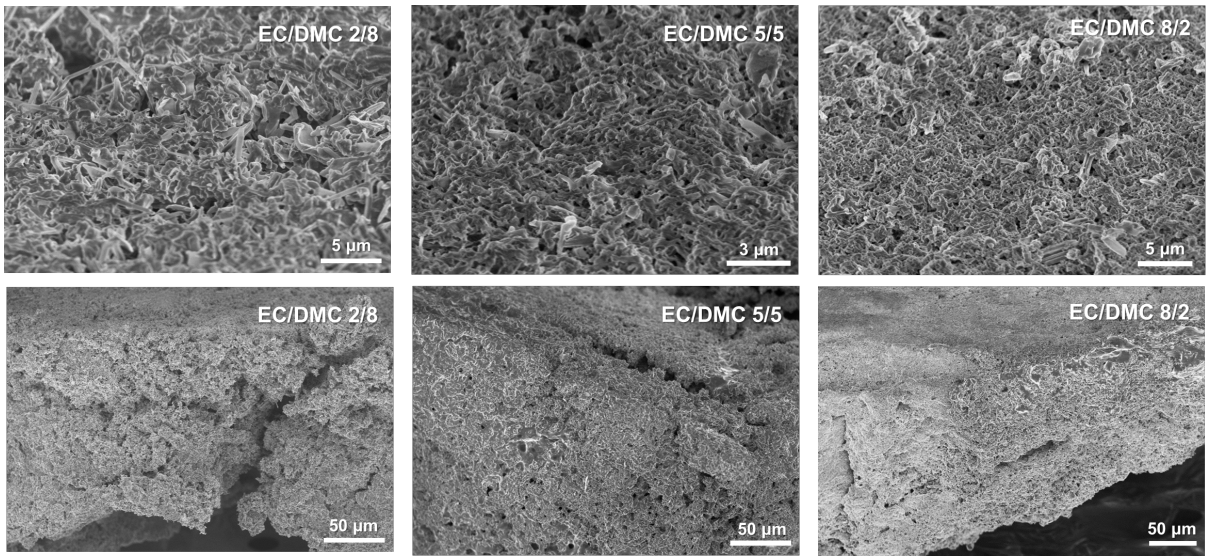
EC/DMC 2/8
5 µm
EC/DMC 5/5
3 µm
EC/DMC 8/2
5 µm
EC/DMC 2/8
50 µm
EC/DMC 5/5
50 µm
EC/DMC 8/2
50 µm

Figure 4

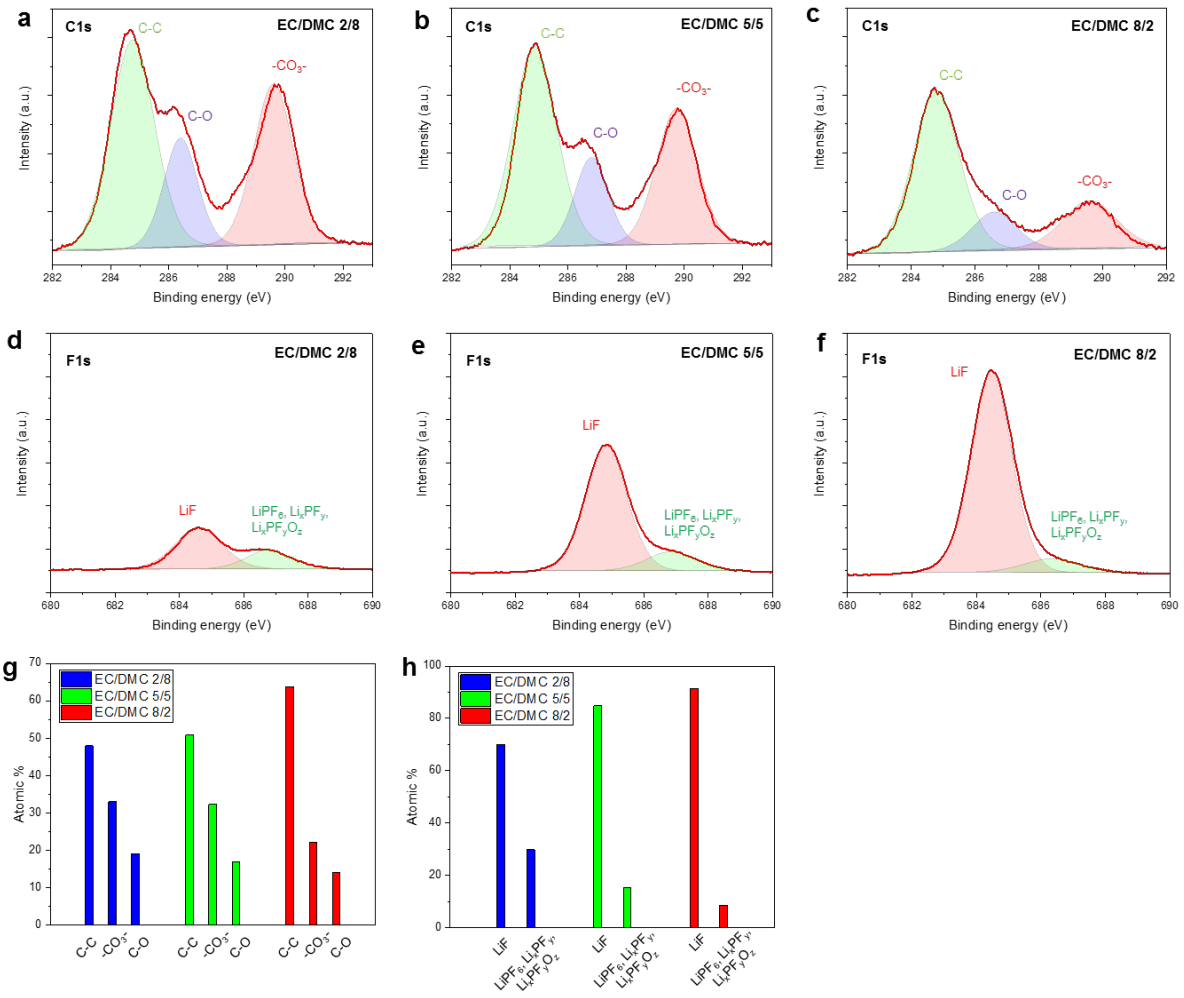
a
C1s
EC/DMC 2/8
C-C
C-O
-CO3-
Intensity (a.u.)
Binding energy (eV)
b
C1s
EC/DMC 5/5
C-C
C-O
-CO3-
Intensity (a.u.)
Binding energy (eV)
c
C1s
EC/DMC 8/2
C-C
C-O
-CO3-
Intensity (a.u.)
Binding energy (eV)
d
F1s
EC/DMC 2/8
LiF
LiPF6, LixPFy, LixPFyOz
Intensity (a.u.)
Binding energy (eV)
e
F1s
EC/DMC 5/5
LiF
LiPF6, LixPFy, LixPFyOz
Intensity (a.u.)
Binding energy (eV)
f
F1s
EC/DMC 8/2
LiF
LiPF6, LixPFy, LixPFyOz
Intensity (a.u.)
Binding energy (eV)
g
EC/DMC 2/8
EC/DMC 5/5
EC/DMC 8/2
Atomic %
C-C
-CO3-
C-O
h
EC/DMC 2/8
EC/DMC 5/5
EC/DMC 8/2
Atomic %
LiF
LiPF6, LixPFy, LixPFyOz

Figure 5

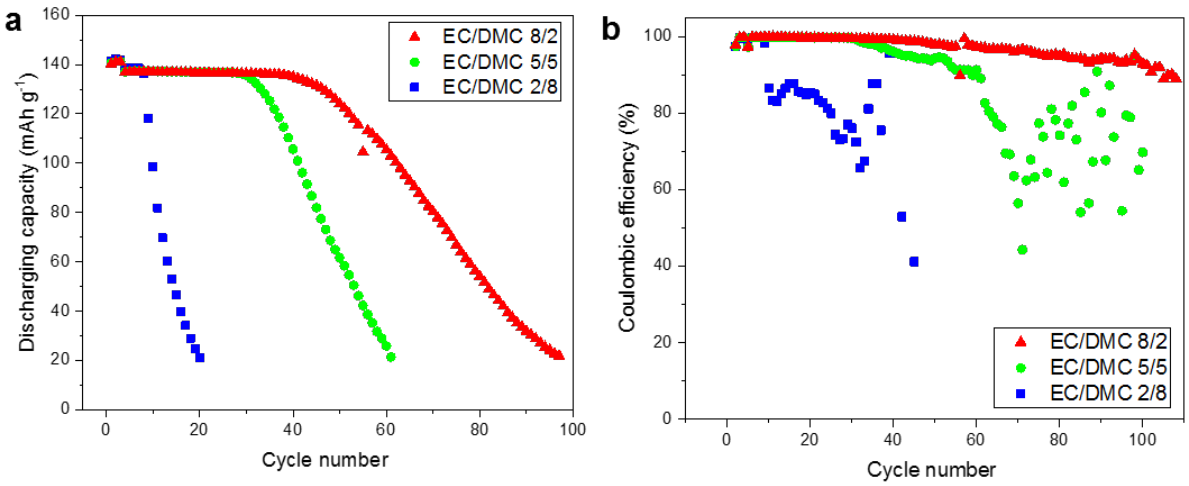
a
Discharging capacity (mAh g-1)
Cycle number
EC/DMC 8/2
EC/DMC 5/5
EC/DMC 2/8
b
Coulombic efficiency (%)
Cycle number
EC/DMC 8/2
EC/DMC 5/5
EC/DMC 2/8